

# Financial multifractality and its subtleties: an example of DAX

A.Z. Górski<sup>1\*</sup>, S. Drożdż<sup>1-4</sup>, J. Speth<sup>3</sup>

<sup>1</sup>*Institute of Nuclear Physics, PL-31-342 Kraków, Poland*

<sup>2</sup>*Institute of Physics, University of Rzeszów, PL-35-310 Rzeszów, Poland*

<sup>3</sup>*Institut für Kernphysik, Forschungszentrum Jülich, D-52425 Jülich, Germany*

<sup>4</sup>*Physikalisches Institut, Universität Bonn, D-53115 Bonn, Germany*

(May 17, 2002)

## Abstract

Detailed study of multifractal characteristics of the financial time series of asset values and of its returns is performed using a collection of the high frequency Deutsche Aktienindex data. The tail index ( $\alpha$ ), the Renyi exponents based on the box counting algorithm for the graph ( $d_q$ ) and the generalized Hurst exponents ( $H_q$ ) are computed in parallel for short and daily return times. The results indicate a more complicated nature of the stock market dynamics than just consistent multifractal.

## I. INTRODUCTION

Comprising the financial time series into a unique description on different time scales by means of the multifractal formalism is an attractive perspective both for fundamental as well as for practical reasons [1]. As a constructive, though also critical, contribution towards this aim in the present paper we systematically review the related basic characteristic of the financial time series using the large collection of the high-frequency Deutsche Aktienindex (DAX) data with over  $10^6$  data records within the time period 28. Nov 1997  $\div$  30. Dec 1999 [2], as well as the daily data since 29. Sep 1959  $\div$  4. Sep 2001 [3] (over  $10^4$  data points). We thus estimate the tail index for the distribution of DAX returns, the Renyi exponents for the DAX index and return's graphs, as well as the corresponding generalized Hurst exponents. It should be stressed that contrary to all the previous related studies the fractal exponents for the graphs are here computed directly, using the (2-dimensional) box counting algorithm, independently of the Hurst exponent computations.

Let  $S(t)$  represent an index value as a function of time. The rate of return within the time lag  $\tau$  (the return time) is usually defined as

$$G'_\tau(t) = \frac{S(t + \tau) - S(t)}{S(t)}. \quad (1)$$

---

\*Corresponding author. Tel.: +48-12-662 8240; fax: +48-12+662 8458. *E-mail address:* Andrzej.Gorski@ifj.edu.pl .

The logarithmic returns

$$G_\tau(t) = \ln S(t + \tau) - \ln S(t) = \ln(1 + G'_\tau(t)) \simeq G'_\tau(t) \quad (2)$$

are more often used when analyzing the financial time series. They are additive with respect to the return time,

$$G_{\tau_1}(t) + G_{\tau_2}(t + \tau_1) = G_{\tau_1 + \tau_2}(t) . \quad (3)$$

This implies translational symmetry of returns and scaling invariance of the asset price (return is identical for prices in any currency). The logarithmic returns are indistinguishable from normal returns if  $|G'_\tau(t)| \ll 1$ . In general, the normal returns (1) are slightly bigger in absolute value which leads to fatter tails due to the inequality  $x > \ln(1 + x)$  for  $x \in (0, 1)$ . Simple index differences have also been investigated but they are dimensional quantities [4]. Throughout this paper by the index  $x_t$  at time  $t$  we will understand the logarithm of its value,  $x_t = \ln S_t$ . Hence, the returns  $G_\tau$  are increments of the index  $x_t$ , just as the white noise (WN) random variables are increments of the Brownian random walk (BRW). The index  $x_t$  can be viewed as integrated returns

$$x_{(t_2+1)\tau} = x_{t_1\tau} + \sum_{k=t_1}^{t_2} G_\tau(k\tau) , \quad (4)$$

where  $x_{t_1\tau}$  is the integration constant. To compare various returns the normalized returns are introduced that have zero average and unit variance

$$g_\tau(t) = \frac{G_\tau(t) - \langle G_\tau(t) \rangle_t}{\sigma(G_\tau(t))} , \quad (5)$$

where  $\langle \dots \rangle_t$  denotes averaging over time variable and  $\sigma(\dots)$  is the standard deviation.

In the following section the probability density function (pdf) of the DAX returns is discussed in order to demonstrate that it shares essentially all the global characteristics identified so far in the literature for other indices, though some small quantitative differences do of course take place. Section III is devoted to study self similarity of the DAX index and of its returns using the (2-dimensional) box counting algorithm. The generalized Hurst exponents are analyzed in Sec. IV. Summary and conclusions are given in the last section.

## II. DISTRIBUTION OF RETURNS

The basic property of normalized returns that has been intensively investigated in recent years is their pdf (obtained by constructing histograms from the empirical data). The old assumption that returns follow the uncorrelated BRW with independent identically distributed (*iid*) Gaussian random variables [5] has been challenged by Mandelbrot and by Fama [6,7]. Mandelbrot analyzed a relatively short (about 2000 data points) time series of cotton prices and he reached conclusion that returns have Lévy stable symmetric distribution with Pareto (power like) fat tails [8,9].

This result has been refined in recent years by the Boston group [10,11] using over  $10^6$  high frequency data points of the S&P500 index. They have found clear departures from the

Lévy stable distribution. First, suggesting the exponential truncation of fat tails for returns  $> 6\sigma$ , where  $\sigma$  is the standard deviation. Later, they found a power law fit with the tail index exceeding the Lévy distribution [11]. The last result was confirmed by other groups for distributions of returns of other indices, including the FOREX data [12].

In this Section we investigate histograms of the DAX returns for high and mid-frequency data. In Fig. 1 we plot the minutely data histogram ( $\tau = 1$  min.) for normalized returns (5). The normalized Gaussian distribution (dotted line) as well as the best fit for the Lévy stable distribution (dashed line) are also plotted. It is clear that the high frequency returns are neither Gaussian nor Lévy stable. The best fit for Lévy distribution within the central region  $g \in [-g_I; +g_I]$ , with  $g_I \simeq 5$  gives for the Lévy parameters  $\alpha = 1.16$  and  $\gamma = 0.286$ . It is interesting to notice that this fit is very stable with respect to the range of the variable  $g$ : one gets identical results within about 1% for  $g_I = 1, 3$  and 10. The tail index ( $\alpha$ ) obtained in this way is too small to fit well for  $g > 2$ . Also, it is smaller than the value 1.4 for S&P500 reported in [11].

Here, one should notice one exception: the central bin contains abundant number of data points (and it was not taken into account for the fits). This phenomenon we call the *zero return enhancement* and it is typical for high frequency data, especially for single stocks, indices that do not contain too many stocks and for not too large stock markets. For short time lags it happens that there are no transactions, the index value is constant and the return distribution is enhanced for the single return value  $g = 0$ . For 15 sec. DAX returns this effects gives about factor 2 enhancement for the central bin and still considerable enhancement for  $\tau = 1$  min. However, for much larger S&P500 index (and larger NY stock market) this effect is hardly visible even for minutely data. Because of this effect and discreteness of returns, we prefer the least square fit adopted for Lévy distribution [13] within the central region of the histogram, with the zero return bin neglected, instead of using the scaling form of the return probability  $p(0)$  (see also [10] and Sec. IVA in [11]).

The log-log plot corresponding to Fig. 1 is given in Fig. 5(A). For comparison the dashed line with slope corresponding to the tail index  $\alpha = 2.4$  is also plotted. We can see that both, negative and positive returns give approximately the same tail index close to the value given above. This value considerably exceeds the range of the Lévy stable distributions. Our estimates give  $\alpha \simeq 2.5$ , in particular  $\alpha = 2.4$  for positive and  $\alpha = 2.6$  for negative returns. Here, one can observe an effect that is reverse to what was found in other markets: the negative return tail has over 8% bigger exponent than the positive tail. Quality of the linear fit for the  $n$  data points with coordinates  $(x_i, y_i)$  is usually measured by the linear correlation coefficient  $r$  (also known as the Pearson's  $r$ ), where  $r \in \langle -1, +1 \rangle$ . For  $r = 1$  the fit is of course perfect. Here, in both cases the correlation coefficient  $r > 0.996$  within the range  $2 < g < 20$ . The resulting tail index,  $\alpha$ , is considerably below the S&P500 result ( $\alpha \simeq 2.8$ ), reported in [11] (though, in both cases well above the Lévy stable limit  $\alpha = 2$ ). In practical terms the DAX develops somewhat fatter tails which reflects its more sizable fluctuations (more "rare events").

For  $g > 20$  (or  $\log_2 g \geq 4.5$ ) the bins of the histogram contain very few data points ( $0 \div 3$  for reasonable bin width that is  $\simeq 0.1$  for Fig. 5(A)) and any regression for those rare events is rather doubtful. Hence, any fit for the very far tail ( $g > 20$ ) truncation seems to be not well justified even for the largest sets of the high frequency data available today. The same results have been also obtained for  $\tau = 15$  sec. In summary, the high frequency DAX return

distribution appears to be quite complicated consisting of the zero return enhancement in bin with  $g = 0$ , Lévy like distribution in the central region ( $|g| \leq 2$ ) with  $\alpha \simeq 1.3$ , inverse power like behavior with  $\alpha \simeq 2.4$  for the tail ( $2 < g < 20$ ) and not easily quantifiable behavior for very large events ( $g > 20$ ).

The above picture, with two different  $\alpha$ 's for the central region and the tail, seems to be consistent with recent suggestions that the return distribution is a union of different distributions for returns in "normal" day time and "rush hours", like soon after opening, before closing and at 14:30 in Europe [14–17]. In this paper we however do not extract special subsets of our financial time series that would screen out such effects as they constitute an essential element of the stock market dynamics. Doing so would also shrink the data set which even as a whole seems to be of relatively modest size (see *e.g.* [18]). Furthermore, in addition to trends in the special subsets mentioned above there exist some other trends on various time-scales which are not connected with the calendar time but are associated with the internal market dynamics (bubbles and crashes, see [19,20] for a recent discussion). Hence, throughout this paper we analyze the complete DAX data set available.

Increase in the return time,  $\tau$ , leads to the increase of the parameter  $\alpha$  of the fitted Lévy curve. In Figs.2,3 and Figs.5(B,C) the same plots as in Figs.1,5(A) are displayed but for return times  $\tau = 10$  min. and  $\tau = 1$  hour, respectively. In both cases we have good fit of the Lévy distribution in the central region,  $g \in (-g_I, +g_I)$ ,  $g_I \simeq 3$ . The Lévy parameters  $\alpha$  and  $\gamma$  slowly grow from the values  $\alpha \simeq 1.2$  and  $\gamma \simeq 0.29$  for the minutely returns up to  $\alpha \simeq 1.4$  and  $\gamma \simeq 0.39$  for the hourly returns (see Figs. 1,2,3). At the same time the tail index outside the central region grows from  $\alpha = 2.4$  for the minutely returns up to  $\alpha \simeq 3.5$  for hourly returns (see Figs. 5(A–C)).

For return times longer than  $\tau = 60$  min. the number of data points is decreasing below  $10^3$  which is not sufficient to precisely estimate the tail behavior. Hence, for mid-frequency data we use much longer data set [3] with historical daily data to have reasonably long time series ( $> 10^3$ ). The return time here,  $\tau \simeq 500$  min., is over 3 orders of magnitude longer than for the shortest available ( $\tau = 15$  sec.) data. Again, the central region where the histogram can be well approximated by a Lévy stable distribution is:  $|g| < g_I \simeq 3$ . The best fit for the Lévy parameters in this region (also, quite stable with respect of the changes in  $g_I$ ) is:  $\alpha \simeq 1.7$  and  $\gamma \simeq 0.385$  (see Fig. 4). In the lower panel, we have added 40-fold magnified tail to show that even for the largest available set of data the tail behavior cannot be reasonably estimated already for  $g > 5$ . For longer return times the situation is even worse. For  $\tau = 30$  min. the tail index seems to be stabilized at the hourly return value  $\alpha \simeq 3.5$  (Fig. 5(D)). In all cases it is greater than the maximum value allowed for the Lévy stable distributions ( $\alpha < 2.0$ ), in agreement with what was found for other indices.

Good fit of the Lévy stable distribution within the central region is consistent with the old result obtained by Mandelbrot for a data set of quite modest size [6]. However, change of the Lévy parameters with the return time ( $\tau$ ), as well as differences in the value of the Lévy parameter  $\alpha$  for the central region and for the tail in each case clearly shows the complexity of the return distributions and their incompatibility with a plain Lévy curve. Also, from lower panel of Fig. 4 one can see apparent difference in the tail behavior of the normalized return distributions and the normalized Gaussian distribution.

The behavior of rare events (*i.e.* for tail with normalized returns  $g > 20$ ) cannot be reasonably estimated for return times  $\tau > 1$  min., at least using the standard histogram

building and fit method, due to the insufficient number of such events in the present day financial data available. Similarly as for the S&P500 [11], even though on short time scales the DAX return distributions are clearly not Lévy stable, in the range from  $\tau = 1/4$  min. up to  $\tau = 1$  day we do not observe convergence of the pdf to the Gaussian (see Figs. 1–4).

For the standard (Lindeberg) version of the Central Limit Theorem (CLT) the random variables must be *iid* and the stochastic process must be stationary. This condition is not satisfied for financial time series where, in particular, various short as well as long range cycles are present. In particular, empirical data display clear nonstationarity as can be seen from the pattern of the recurrence plot that is given for 10 min. returns data series in Fig. 6. Here, the relation between closeness in time and in phase space is displayed using the Takens phase space reconstruction method. The embedding dimension is taken  $E = 5$ , but its exact value is not important in this case as the recurrence plot is not sensitive with respect to this parameter. The normalized neighborhood size was set  $\varepsilon = 0.2$ , but similar structures were obtained for smaller  $\varepsilon$  (see *e.g.* [21] Sec. III and [22,23] for more details), as well as for the embedding dimension up to  $E = 9$ . Recently, Bouchaud *et al* [24] have shown that for a special model with correlations similar as in financial series a slow convergence to the Gaussian pdf can be proven and it is visible for return times  $\tau > 1$  day (see also [11]).

### III. SELF SIMILARITY

Distribution of returns gives us only a small part of the whole information included in the time series. In particular, the time order is completely neglected. To account for the time dependence one should analyze the whole (2–dimensional) graph of the functions  $x_t = x(t)$  and  $g_\tau(t)$  ( $D_G$  in the notation of [1]). Although, the projections of the data points at the time and at the value axis are pseudofractal sets with zero Hausdorff–Besicovitch dimension and their pseudofractal scaling exponents are equal to one [25], the graph in principle can be a regular fractal as is the case for the WN and BRW. The fractal properties of returns have been suggested long ago by Mandelbrot [26]. More detailed analysis has been published by Evertsz *et al* [12,27]. However, it should be stressed that their analysis was based on the calculation of the generalized Hurst exponents (see Sec. IV).

To investigate fractal properties of DAX index and its returns we apply directly the standard box counting algorithm for computation of the Renyi box counting exponents defined by [28]

$$d_q = \frac{1}{1-q} \lim_{N \rightarrow \infty} \frac{\ln \sum_i p_i^q(N)}{\ln N} \equiv \lim_{N \rightarrow \infty} \frac{\ln Y(N)}{\ln N}, \quad (6)$$

where  $N$  is the total number of "boxes" (bins),  $p_i$  is the part of the "mass" (*i.e.* fraction of all points) contained in the  $i$ -th box.

Computation is performed for both graphs,  $x(t)$  and  $g_\tau(t)$ . To the best of our knowledge this is the first direct calculation of the fractal dimensions of the graphs for any financial index and its returns. Usually, the self similar properties were inferred from the Hurst exponents or from the rescale range analysis, see *e.g.* [29,30]. As will be shown in the following sections these two methods give different results, especially for the returns' graphs. In Fig. 7 results of the calculations of  $d_q$  exponents are displayed for the logarithm of DAX ( $x_t$ ). The calculations for time lags  $\tau = 1, 10, 60$  min., 1 day and for  $q = 0.5, 1, 2$  and 4

are shown. In fact, the same results were obtained for the plain index ( $S_t$ ). This supports the view that the graph is a real fractal, not just a pseudofractal as the exponents for fractals are invariant with respect to the homeomorphic transformations. In all cases one gets quite reasonable linear fits. The correlation parameter ( $r$ ), as can be expected, is lowest for  $\tau = 60$  min, where the number of original data points is the smallest (below  $10^4$ ). However, even in this case we have  $r > 0.998$  (for all other cases we have  $r > 0.9994$ ), quite a reasonable value. The linear scaling extends through  $6 \div 9$  points (binary orders of magnitude) at the log–log plot which is also a standard range for numerical estimates of fractal dimensions. The resulting Renyi box counting exponents are given in Table I. Even though, the range of the return time ( $\tau$ ) and the range of the index  $q$  are relatively large, all values for the exponents  $d_q$  are within the interval  $d_q \in [1.3, 1.4]$ , well below the value characteristic for the BRW (in all Tables the last digit is not the significant digit). This suggests that we have a self similar and close to monofractal curve for the DAX index. In addition, one can observe a general tendency that the index  $d_q$  is slowly decreasing for longer time lags except for  $\tau = 1$  day, where another set of data was used.

Similar analysis applied to the normalized DAX returns leads to the result displayed in Fig. 8. Here, the quality of the linear fit in the log–log plot is not as convincing as in the previous case (Fig. 7) of the index itself, especially for the smaller  $q$ -values. Extracting nevertheless the corresponding linear best fit ( $r > 0.994$ ) coefficients results in the values for  $d_q$  which are more dispersed and spread within the range  $d_q = 1.4 \div 1.7$ , depending on  $q$  as well as on the return time,  $\tau$ .

Our results thus indicate that, within a few percent, which is comparable to the estimated numerical accuracy, the  $q$ -dependence (and  $\tau$ -dependence) of  $d_q$  is rather weak. Hence, the corresponding graphs can be viewed as close to monofractal and this indication is especially suggestive for the index whose scaling properties are quite convincing. It is also worth to notice that the corresponding  $d_q$  values for the index are systematically below the BRW value (1.5). This may reflect an important element specific to the financial dynamics. Somewhat less transparent is the related scaling behavior of the returns, though this behavior also carries some information about the underlying dynamics and is therefore shown here. Assuming however that some scaling approximately applies in this case as well, it seems natural that the above estimated bounds limiting variation of  $d_q$  for returns point to values which are systematically bigger than for the index, as the former is the differentiated index (see eq.(4)). While this difference equals 0.5 for WN and BRW, in our case the difference is on average significantly smaller. To avoid numerical artifacts we have repeated all calculations with logarithm of the index and we have obtained the same results within the numerical accuracy. This shows that the results are invariant with respect to nonlinear transformations of the data. As the fractal dimensions and Renyi box counting exponents are related to the Hurst exponents we will return to this issue in the subsequent section.

#### IV. GENERALIZED HURST EXPONENTS

The Hurst exponent ( $H_1$ ) has been introduced long ago in the "rescale range theory" for measurements of the Nile flooding and drought amplitudes [31]. The generalized Hurst exponents,  $H_q = H(q)$ , for a time series  $g(t)$  ( $t = 1, 2, \dots$ ) are defined by the scaling properties of its structure functions  $S_q(\tau)$  [1]

$$S_q(\tau) = \langle |g(t + \tau) - g(t)|^q \rangle_T^{1/q} \sim \tau^{H(q)} \quad (7)$$

where  $q > 0$ ,  $\tau$  is the time lag and averaging is over the time window  $T \gg \tau$ , usually the largest time scale of the system. The function  $H(q)$  contains information about averaged generalized volatilities at scale  $\tau$  (only  $q = 1, 2$  are used to define the volatility). In particular, the  $H_1$  exponent indicates persistent ( $H_1 > 1/2$ ) or antipersistent ( $H_1 < 1/2$ ) behavior of the trend. For the BRW (brown noise,  $1/f^2$ ) one gets  $H_q = 1/2$ , while for the pink ( $1/f$ ) and WN we have  $H_q = 0$ . For the popular Lévy stable and truncated Lévy processes with parameter  $\alpha$  it has been found that  $H_q = q/\alpha$  for  $q < \alpha$  and  $H_q = 1$  for  $q \geq \alpha$  [32].

The direct computation of the generalized Hurst exponents was performed for return times  $\tau = 1, 10$  and  $60$  min. as well as for  $\tau = 1$  day (as for the generalized Renyi exponents of the graphs) and for the index  $q = 0.5, 1.0, 2.0$  and  $4.0$ . The value  $q = 0$  cannot be used, as  $q > 0$  (see eq. (7)). Computation of  $H_q$  for the DAX index is displayed in Fig. 9. The linear scaling in the log-log plot is here excellent and the corresponding results are collected in Table II. One can clearly see that  $H_q$  decreases with increasing  $q$ , though this effect is smaller for longer time lags. Also, for the smaller  $q$ -values it decreases with the increasing return time  $\tau$ , at least within the range  $\tau = 1 \div 30$  min., and the process is persistent ( $H_1 > 1/2$ ). Very interestingly however, for the larger  $q$ -values this tendency gets reversed:  $H_4(\tau)$  can be seen to approach the BRW limit from below assuming values significantly lower than  $1/2$  at the high-frequencies. For  $\tau \simeq 10$  min. the exponent  $H_1$  approaches the BRW value,  $1/2$ . Notice, that at around  $\tau_c \simeq 30$  min. the tail index is also stabilized (see Sec. II). Similar critical value of  $\tau$  was also reported for S&P500 index in [11] and estimated  $\tau_c \simeq 20$  min. (from (7) it is clear that the structure function  $S_2(\tau)$  of the index is equivalent to the volatility  $v(\tau)$ ). Hence, the correlations cease to exist slightly faster for DAX. This may indicate that the correlations are weaker in the smaller market. Also, for high frequency data the  $q$ -dependence is much stronger. When  $\tau$  grows, crossing the critical value  $\tau_c$ ,  $H_q$  becomes almost independent of  $q$ .

For completeness we have performed the same computation for the DAX returns. The quality of the linear scaling in this case is not as excellent as for the index itself but still it quite consistently points to  $H_q \simeq 0.0$  for all the calculated values of  $q$  and  $\tau$ , the same result as for the WN (in contrast to the index that considerably differs from BRW). This difference may be explained by the existence of stronger correlations for the index.

## V. DISCUSSION AND SUMMARY

The financial processes are governed by a complex dynamics with many degrees of freedom and various additional noise terms due to complicated interactions with the external environment. This is a non-stationary evolutionary process with strong correlations, to large extent resembling biological evolution, and it cannot be viewed as an equilibrium process [33]. From this perspective it is not very surprising that the formalism that is so far available may not yet offer an optimal scheme to consistently comprise all the related effects. The present paper constitutes an attempt to provide some further relevant empirical characteristics for another important world stock market, the Deutsche Aktienindex, in addition to what already is available in the literature. Several such characteristics, not always easy to interpret, are identified.

In particular, the returns' pdf displays Pareto (fat) tails of the type  $1/x^\alpha$ . As was shown in Sec. II the distribution of the DAX returns has its central part close to the Lévy distribution with  $\alpha$  from 1.2 (minutely returns) up to  $\alpha \simeq 1.7$  (daily returns). Within the "tail region", *i.e.* for returns greater than 3 but below  $10 \div 20$  standard deviations, a simple linear regression implies the tail index  $\alpha \simeq 2.4$  for minutely returns and up to  $\alpha \simeq 3.5$  for daily returns. The available data sets seem to be too small to calculate (with reasonable certainty level) the tail behavior beyond  $10 \div 20$  standard deviations. We find various tail indices for various regions of the distribution, for different return times and for different financial indices (see *e.g.* [11] for comparison). There is no doubt that the power like behavior plays important role, but its manifestations are more complex than it was originally assumed. It is worth to mention that similar multiscaling of pdf was found in a monofractal toy model discussed by Bouchaud *et al* [24].

From the dynamical point of view more important than pdf are Hurst and Renyi exponents of the index and returns' graph. This is because they take into account the time dependence of the process. Therefore, the main part of our analysis was devoted to study these quantities. For regular (mono-) fractal set the following simple relation between fractal exponent of the graph ( $d_0$ ) and the Hurst exponent is often satisfied [1,29,30,34]

$$d_0 = 1 + E - H_1 \quad (8)$$

where  $E$  is the embedding dimension of the data series ( $E = 1$  for a one dimensional data). In particular, this relation is preserved for the WN, for the BRW as well as for the Weierstrass–Mandelbrot fractal [35] and for any fractional Brownian motion [1]. This relation is usually used when discussing the fractal behavior of financial indices. However, the often cited relation (8) is not fulfilled in our case. In general, the multifractal formalism for a function, instead of the exact spectrum, yields an upper bound of its Hölder spectrum [1,34]. Hence, in principle it is necessary to calculate the Renyi exponents by direct application of the box counting algorithm for the graphs.

We have used the (2-dimensional) box counting algorithm to calculate the fractal properties of the financial graphs. The Renyi exponents with  $q = 0.5, 1.0, 2.0$  and  $4.0$  for the DAX index were found to be around 1.3, slowly decreasing with growing  $q$  (about 15% below the constant BRW value, 1.5). However, for the DAX returns the corresponding values turn out not to be so precisely determined due to a somewhat poorer scaling but still can be localized within the range  $1.4 \div 1.7$ , more below the WN value and with stronger  $q$ -dependence. The decrease of  $d_q$  with growing  $q$ , usually viewed as a sign of multifractality, is bigger here than for the index itself, especially for the high-frequency data (1 min. returns). It is worth to notice that the estimated difference between the fractal exponents of the index and exponents of the corresponding differential series (returns) is only about  $0.2 \div 0.3$ , while it is exactly equal to 0.5 for the BRW and WN. As a potential most visible and significant difference between the behavior of the financial index and BRW, this effect demands however further more systematic study. Comparing the above results with the calculated Hurst exponents one can also see that the relation (8) is violated for the index and seems to be violated even more for the returns. In contrast to the Renyi exponents, the generalized Hurst exponents for returns are compatible with those of the WN (equal to zero). For the index we obtain persistent behavior ( $H_1 = 0.51 \div 0.63$ ) which is slightly stronger for short time lags. Here, the  $q$ -dependence is also stronger than for the  $d_q$ .

One can conclude that the DAX data series, both for the (logarithm of) index and its returns, have very complicated self-similar structures that may escape any unique multifractal description. One likely reason is that the real financial data series are superpositions of series with different properties, *e.g.* for the "regular" and "rush" hours as was suggested recently [14–17]. To clarify these intriguing effects further empirical and theoretical analysis is necessary.

#### ACKNOWLEDGMENTS

We thank F. Grümmer and J. Kwapien for helpful exchanges. M. Frame and J. Szmigielski of Yale Math. Dept. are acknowledged for clarifying comments concerning fractal and Hurst exponents.

## REFERENCES

- [1] B. Mandelbrot, *Fractals and Scaling in Finance*, Springer, New York, 1997.
- [2] H. Goepl, Data from Karlsruher Kapitalmarktdatenbank (KKMDB), Inst. für Entscheidungstheorie u. Unternehmensforschung, Universität Karlsruhe (TH).
- [3] Data available at <http://biz.yahoo.com/ffc/de/>
- [4] L. Gillemot, J. Töyli, J. Kertesz, K. Kasaki, *Physica A* 282 (2000) 304.
- [5] L. Bachelier, *Ann. Sci. de l'Ecole Norm. Sup.* III–17 (1900) 21.
- [6] B. Mandelbrot, *J. Business* 36 (1963) 294.
- [7] E.F. Fama, *J. Business* 36 (1963) 420.
- [8] P. Lévy, *Calcul des probabilités* Gauthier–Villars, Paris, 1925; *Théorie de l'addition des variables aléatoires*, Gauthier–Villars, Paris, 1934.
- [9] V. Pareto, *Cors d'Economie Politique*, Lausanne & Paris, 1897.
- [10] R.N. Mantegna, H.E. Stanley, *Nature* 376 (1995) 46.
- [11] P. Gopikrishnan, V. Plerou, L.A.N. Amaral, M. Meyer, H.E. Stanley, *Phys. Rev. E* 60 (1999) 5305.
- [12] C.J.G. Evertsz, *Proc. of First Int. Conf. on High Frequency Data in Finance* (Zürich 1995).
- [13] J.E. Dennis, D.M. Gay, R.E. Welsch, *ACM Trans. Math. Software* 7 (1981) No 3.
- [14] Z.F. Huang, *Physica A* 287 (2000) 405.
- [15] S. Drożdż, J. Kwapien, F. Grümmer, F. Ruf, J. Speth, *Physica A* 299 (2001) 144.
- [16] J. Kwapien, S. Drożdż, F. Grümmer, F. Ruf, J. Speth, *Decomposing the stock market intraday dynamics*, arXiv:cond-mat/0108068, *Physica A*, in print.
- [17] E.C.J. Huppert, A.J. Menkveld, *J. Fin. Markets* 5 (2002) 57.
- [18] R. Weron, *Int. J. Mod. Phys. C* 12 (2001) 206.
- [19] A. Johansen, D. Sornette, *Physica A* 294 (2001) 465.
- [20] S. Drożdż, F. Ruf, J. Speth, M. Wójcik, *Eur. Phys. J. B* 10 (1999) 589.
- [21] R. Hegger, H. Kantz, Th. Schreiber, *Chaos* 9 (1999) 413.
- [22] J.P. Eckmann, S.O. Kamphorst, D. Ruelle, *Europhys. Lett.* 4 (1987) 973.
- [23] Th. Schreiber, *Phys. Rep.* 308 (1998) 1.
- [24] J.-P. Bouchaud, M. Potters, M. Mayer, *Eur. Phys. J. B* 13 (2000) 595.
- [25] A.Z. Górski, *J. Phys. A* 34 (2001) 7933.
- [26] B.B. Mandelbrot *The fractal geometry of nature*, San Francisco, Freeman, 1982.
- [27] C.J.G. Evertsz, K. Berkner, *Chaos, Solitons & Fractals* 6 (1995) 121.
- [28] A. Renyi, *Probability Theory*, Amsterdam, North–Holland, 1970.
- [29] J.A. Skjeltrop, *Physica A* 283 (2000) 486.
- [30] M. Ausloos, *Financial time series and Statistical mechanics*, in: *Vom Billardtisch bis Monte Carlo — Spielfelder der Statistischen Physik*, eds. K.H. Hoffmann, M. Schreiber, Springer, Berlin, 2001 (arXiv:cond-mat/0103086).
- [31] H.E. Hurst, *Trans. of the Am. Soc. of Civil Engineers* 116 (1951) 770; H.E. Hurst, R.P. Black, Y.M. Simaika, *Long Term Storage*, Constable, London, 1965.
- [32] D. Schertzer, S. Lovejoy, F. Schmidtt, Y. Chigirinskaya, D. Marsan, *Fractals* 5 (1997) 427.
- [33] J.L. McCauley, *Physica A* 299 (2001) 294.
- [34] S. Jaffard, *SIAM J. Math. Anal.* 28 (1997) 994; 971.
- [35] M.V. Berry, Z.V. Levis, *Proc. Roy. Soc. Lond. A* 370 (1980) 459.

TABLES

TABLE I. Renyi box counting exponents ( $d_q$ ) for DAX index

| $\tau$  | $q = 0.5$ | $q = 1$ | $q = 2$ | $q = 4$ |
|---------|-----------|---------|---------|---------|
| 1 min.  | 1.38      | 1.36    | 1.34    | 1.30    |
| 10 min. | 1.36      | 1.35    | 1.33    | 1.29    |
| 60 min. | 1.30      | 1.30    | 1.29    | 1.26    |
| 1 day   | 1.33      | 1.33    | 1.32    | 1.29    |

TABLE II. Hurst exponents ( $H_q$ ) for DAX index

| $\tau$  | $q = 0.5$ | $q = 1$ | $q = 2$ | $q = 4$ |
|---------|-----------|---------|---------|---------|
| 1 min.  | 0.66      | 0.63    | 0.56    | 0.33    |
| 10 min. | 0.52      | 0.51    | 0.48    | 0.36    |
| 60 min. | 0.57      | 0.55    | 0.51    | 0.44    |
| 1 day   | 0.52      | 0.52    | 0.51    | 0.46    |

## FIGURES

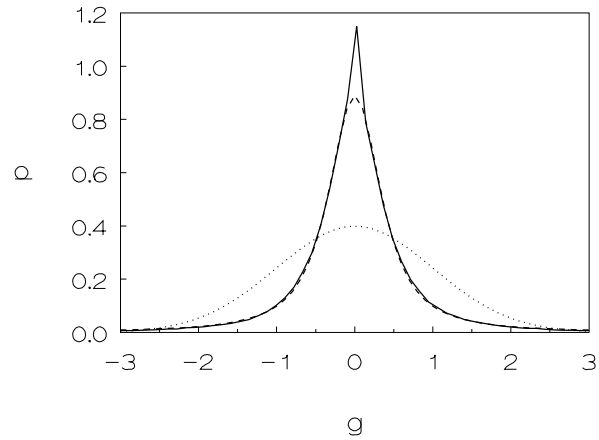


FIG. 1. Histogram for DAX normalized minutely returns. Normalized Gauss (dotted line) and best fit for Lévy stable distribution (dashed line,  $\alpha = 1.16$  and  $\gamma = 0.286$ ) are also displayed.

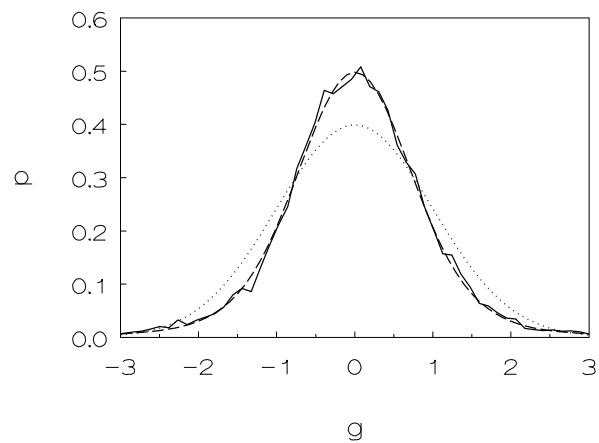


FIG. 2. Histogram for DAX normalized 10 min. returns. Normalized Gauss (dotted line) and best fit for Lévy stable distribution (dashed line,  $\alpha = 1.44$  and  $\gamma = 0.327$ ) are also displayed.

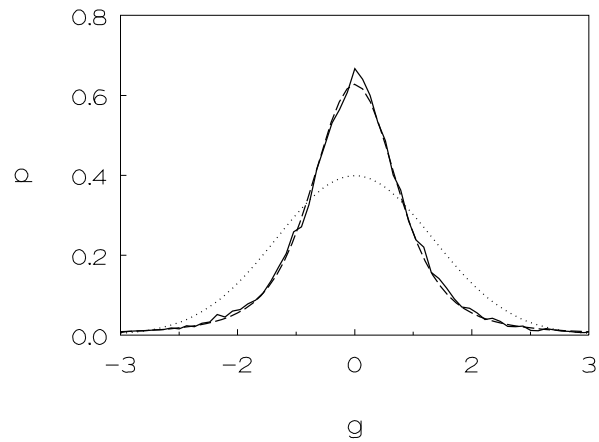


FIG. 3. Histogram for DAX normalized 1 hour returns. Normalized Gauss (dotted line) and best fit for Lévy stable distribution (dashed line,  $\alpha = 1.40$  and  $\gamma = 0.354$ ) are also displayed.

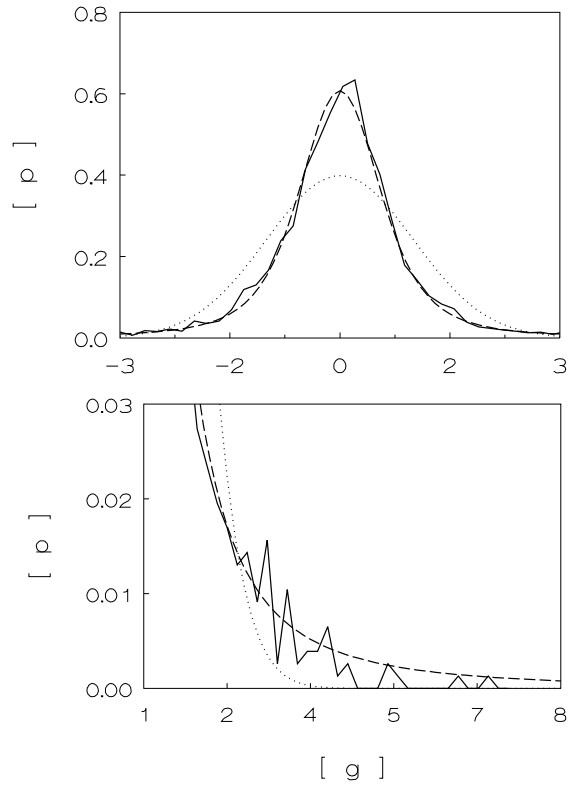


FIG. 4. Histogram for DAX normalized daily returns. Normalized Gauss (dotted line) and best fit for Lévy stable distribution (dashed line,  $\alpha = 1.7$  and  $\gamma = 0.385$ ) are also displayed. Lower panel: magnification of the tail behavior.

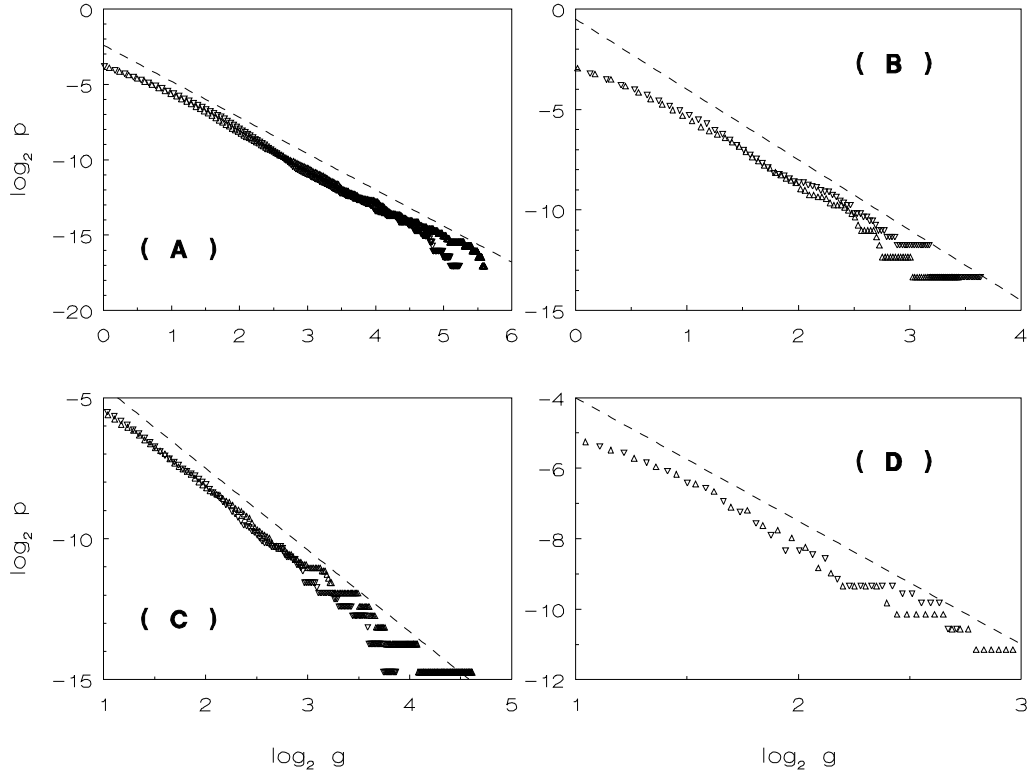


FIG. 5. Log-log plot for normalized minutely DAX returns for return times = 1, 10, 60 min. and 1 day, respectively for plots (A–D). The triangles represent positive tail while the inverted triangles, the negative tail. The dashed line corresponds to the tail index  $\alpha = 2.4, 2.9, 3.5$  and  $3.5$  for graphs (A–D).

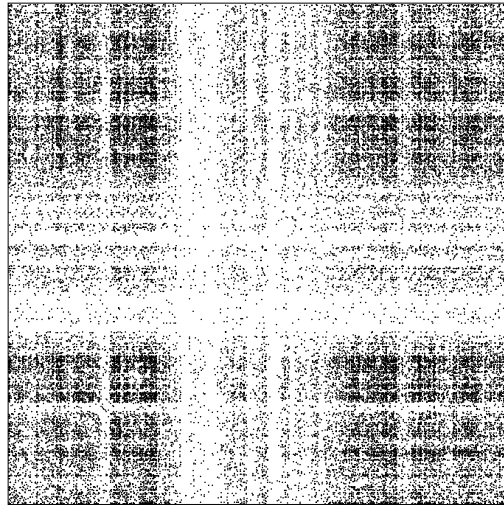


FIG. 6. Recurrence plot for DAX 10 min. returns. Time is on both axis, the embedding dimension is set to  $E = 5$  and the normalized neighborhood size is  $\varepsilon = 0.2$ .

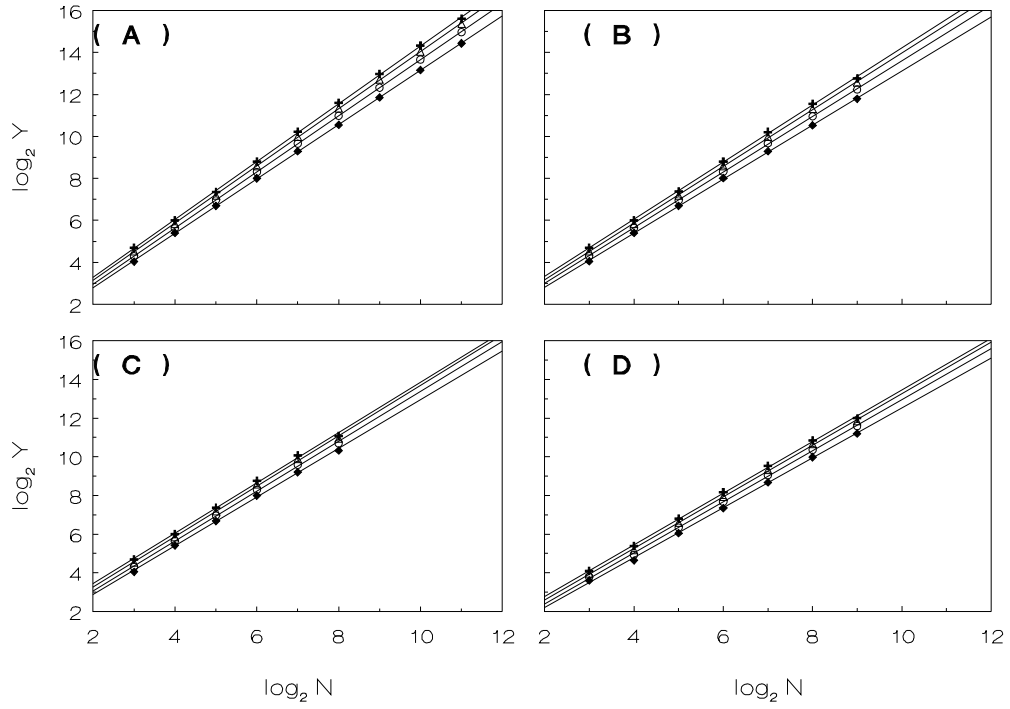


FIG. 7. Calculating Renyi box counting exponents,  $d_q$ , for log of DAX.  $q = 0.5, 1, 2, 4$  for crosses, triangles, circles, and diamonds, respectively. Plots from A to D are given for return times  $\tau = 1, 10, 60$  min. and 1 day. Solid lines represent least square linear fits.

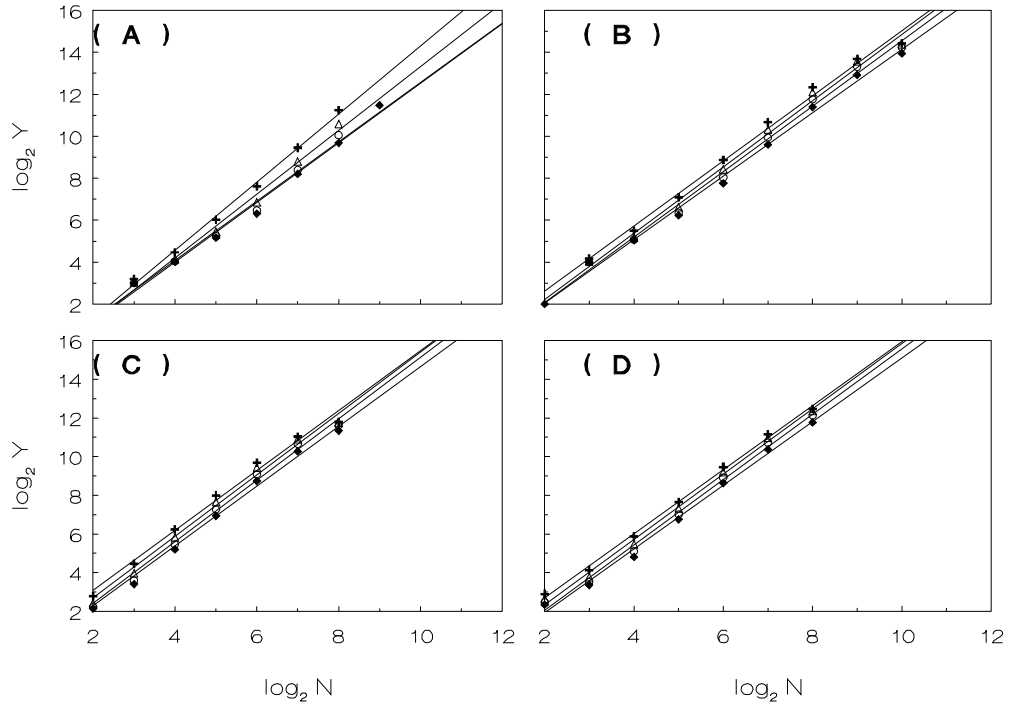


FIG. 8. Calculating Renyi box counting exponents for DAX returns.  $q = 0.5, 1, 2, 4$  for crosses, triangles, circles, and diamonds, respectively. Plots from A to D are given for return times  $\tau = 1, 10, 60$  min. and 1 day. Solid lines represent least square linear fits.

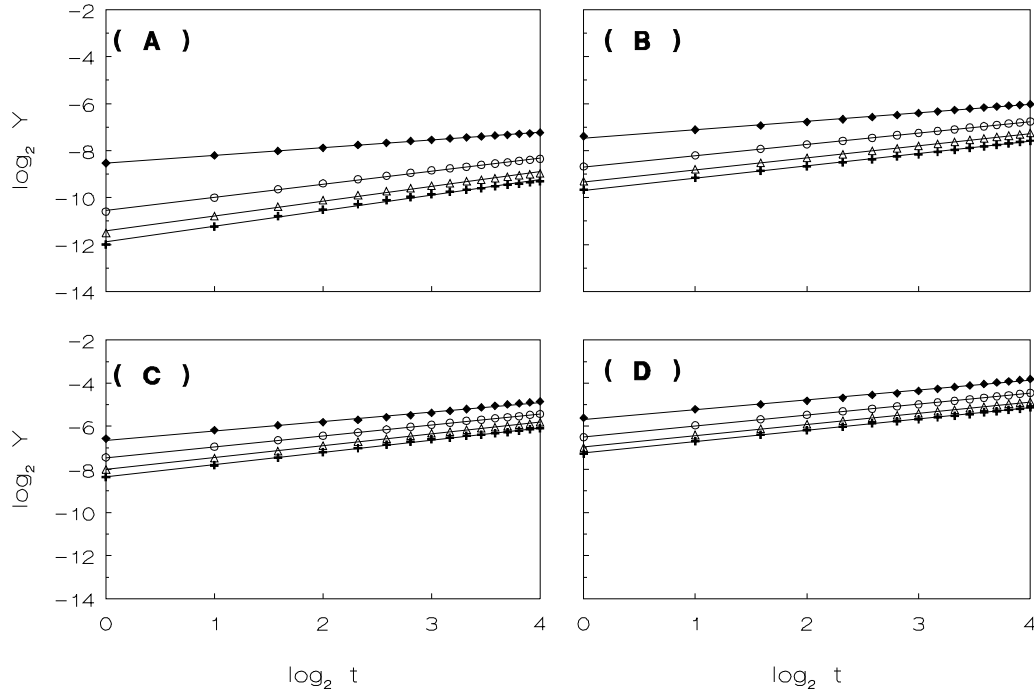


FIG. 9. Calculating generalized Hurst exponents for DAX index.  $q = 0.5, 1, 2, 4$  for crosses, triangles, circles, and diamonds, respectively. Plots from A to D are given for return times  $\tau = 1, 10, 60$  min. and 1 day. Solid lines represent least square linear fits.